J. L. H. Mik, B. M. Sparkes, C. Perrella, P. S. Light, S. Ng, A. N. Luiten, and D. J. Ottaway

High-transmission fiber ring resonator for spectral filtering of master oscillator power amplifiers

OSA Continuum, 2019; 2(8):2487-2495

DOI: http://dx.doi.org/10.1364/OSAC.2.002487

Research Article | Vol. 2, No. 8 / 15 August 2019 / OSA Continuum 2487

OSA CONTINUUM

High-transmission fiber ring resonator for spectral filtering of master oscillator power amplifiers

J. L. H. MIK,[1,2] B. M. SPARKES,[1,*] C. PERRELLA,[1] P. S. LIGHT,[1] S. NG,[1,2] A. N. LUITEN,[1] AND D. J. OTTAWAY[1,2]

[1]*The University of Adelaide, Institute for Photonics & Advanced Sensing (IPAS), School of Physical Sciences, Adelaide, SA 5005, Australia*
[2]*ARC Centre of Excellence for Gravitational Wave Discovery (OzGrav), University of Adelaide Node, Adelaide, SA 5005, Australia*
[*]*ben.sparkes@adelaide.edu.au*

Abstract: We experimentally characterize a fiber-based ring resonator constructed from two commercially available 2x2 polarization-maintaining directional couplers. This ring resonator has a maximum noise suppression of 25 dB and resonant transmission of 80% at 1550 nm. Its high transmission means this ring resonator is ideally suited for the spectral filtering of master oscillator power amplifier light sources in a robust, compact, and all-fiber package. The limits of such a ring resonator for use in gravitational-wave detectors are discussed, and we show how it could be used to filter the low-power amplifier section and reduce the noise suppression requirements for the final free-space mode-cleaner.

1. Introduction

High power lasers that simultaneously possess high spatial stability and low noise are required in numerous applications including lidar [1], optical communications [2–4], trapped ion quantum computing [5,6] and advanced gravitational-wave (GW) detection [7]. Fiber lasers are particularly well suited to these tasks as they inherently deliver single mode emission from a compact and robust source, while minimizing the need for complex alignment procedures [8]. The maximum power that can be emitted from a single frequency fiber-based laser is only a few hundred milliwatts [9]. For applications requiring higher power, a low power master laser can be amplified by a series of increasingly powerful laser amplifiers, i.e., a master oscillator power amplifier (MOPA) configuration [10]. In this situation, amplified spectral emission (ASE) noise can significantly degrade the spectral quality of the output.

Advanced GW detectors place extremely stringent requirements on the spectral purity of high power light sources. Traditionally, light for GW detectors has been provided by bulk lasers, with severe filtering needed to meet the exacting demands of high spatial mode stability, as well as low intensity noise (170 dBc) at key frequencies in the radio-frequency (RF) band from 10 to 100 MHz [11]. This filtering is currently provided by passive Fabry-Perot (F-P) ring cavities (see Fig. 1(a)(i)) at the end of the amplifier chain [12]. The move towards fiber laser sources has already relaxed the spatial filtering requirements significantly [13]. The RF noise suppression requirements of the final mode-cleaner could similarly be relaxed if the noise on the MOPAs were reduced by including a series of spectral filters situated between each stage of the amplification chain (see Fig. 1(b)) [14]. Such filters would prevent spectral noise on the output of low power stages being amplified, thereby reducing the intensity noise on the amplified output.

In this paper we thoroughly experimentally characterise an efficient fiber-based filter that could be conveniently placed between MOPA stages to greatly reduce the RF noise of the output at key GW detection frequencies. This will allow for the reduction of the required finesse and

#369180 https://doi.org/10.1364/OSAC.2.002487
Journal © 2019 Received 4 Jun 2019; revised 30 Jul 2019; accepted 30 Jul 2019; published 7 Aug 2019

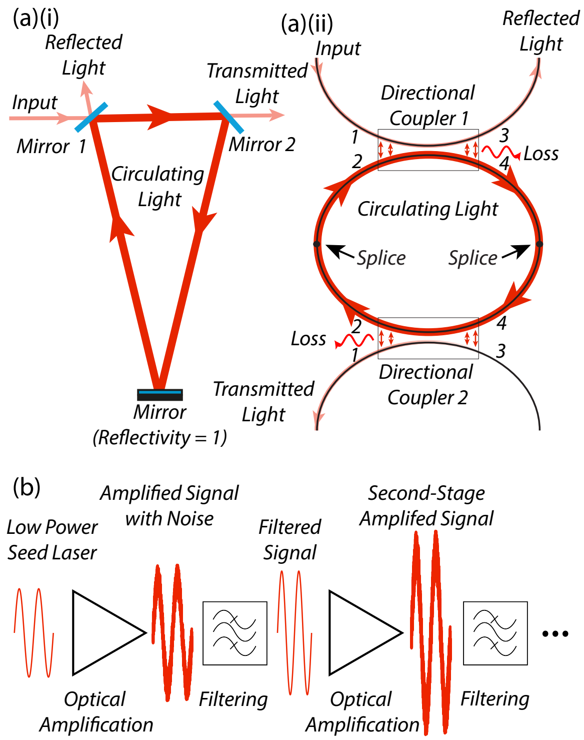

Fig. 1. (a) Operation of (i) a three-mirror Fabry-Perot mode-cleaner and (ii) an equivalent all-fiber ring resonator made from two directional couplers (ports numbered). (b) Illustration of chaining MOPA systems with optical filtering occurring after each step to remove ASE noise.

hence circulating power of the filter cavity placed between the laser output and the suspended interferometer. The mode-cleaner, created with two commercially available directional couplers (DCs - Fig. 1(a)(ii)) demonstrated 25 dB of noise suppression while transmitting 80% of the incident light on resonance, the first time such a ring resonator has provided over 50% efficiency.

2. All-fibre spectral filters

Many forms of fiber-based resonators have been investigated previously due to their desirable properties. For instance, all-fiber resonators can be produced from fiber Bragg gratings (FBGs) [15,16]. However, the linear geometry of a FBG-based resonator intrinsically generates significant back reflections, and it is therefore not desirable to use them in a chain without the introduction of additional components and, therefore, complexity.

An alternative method is a fiber ring resonator, where a single DC is used to form a fiber loop. A combination of fiber and DCs have been used to produce notch filters, narrow-band fiber ring lasers, frequency selective devices and rotation sensors [17–20]. These approaches are not suitable, however, for suppressing broad spectral noise, such as that produced by ASE.

An extension of the single DC ring resonator is to join two DCs together to form a circulating loop [21,22]. This is equivalent to a three-mirror free-space mode-cleaner, with separate input, reflection and transmission ports, as shown in Fig. 1(a)(ii). The ring geometry of this type of resonator has the advantage of inherent isolation, which protects proceeding stages from destabilising and sometimes dangerous back-reflections. It is also convenient for active frequency stabilisation via the reflection port, removing the need for additional fiber elements such as

OSA CONTINUUM

isolators, circulators or polarization optics. This type of ring resonator has previously been used for spectral filtering [23] and optical frequency comb decimation [24], but the greater than 50% losses achieved to date [24] make these resonators highly undesirable for spectral filtering of amplifier chains, where high transmission is of critical importance.

3. Experimental details and characterisation

To form our high-transmission resonator, we spliced together two commercially available polarization-maintaining, 10 μm core diameter, 90:10 fiber DCs (Newport F-PMC-1550-10), creating a ring resonator of length 2.7 m. Before splicing, we characterised the reflectivity of the DCs, finding $R = 0.90 \pm 0.02$. We used an arc splicer (Fujikura FSM-100P) to join the fibres, with a measured upperbound on the splice loss of 0.01 dB. Port 1 of DC 1 acts as the input to the ring resonator (Fig. 1(a)(ii)), with light injected into this port transferred to Ports 3 (90%) and 4 (10%) of DC1, which act as the reflected and intra-cavity ports of the ring resonator respectively. Light emitted from Port 4 of DC1 will continue to Port 4 of DC2, which is mostly coupled into Port 2 (90%) of DC2, where it continues back to Port 2 of DC1. This completes the loop and sets the resonant condition for constructive interference. Port 1 of DC2 acts as the analogue of the transmitted port of the free-space resonator.

The intensity of light exiting the reflected port (3 of DC1) and transmitted ports (1 of DC2) can be expressed as [25]:

$$I_{\text{reflected}} = \frac{R(1-\mathcal{V})^2 + 4R\mathcal{V}\sin^2(kp)}{(1-R\mathcal{V})^2 + 4R\mathcal{V}\sin^2(kp)} \tag{1}$$

$$I_{\text{transmitted}} = \frac{(1-R)^2\mathcal{V}}{(1-R\mathcal{V})^2 + 4R\mathcal{V}\sin^2(kp)} \tag{2}$$

where R and $\mathcal{V}$ are the average reflectivity and efficiency (i.e., $\mathcal{V} = I_{out}/I_{in} = 1 - \text{loss}$) of each DC including splice loss, p is the perimeter of the fiber loop and $k = 2\pi/\lambda$ is the wave number of the incident light inside the fiber. The finesse, $\mathcal{F}$, relates to reflectivity and loss as $\mathcal{F} = \pi/|\ln(R\mathcal{V})|$

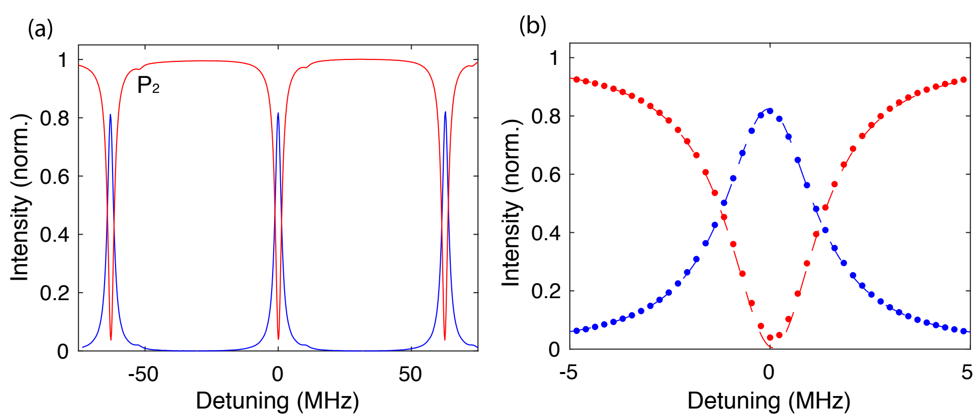

Fig. 2. (a) Transmitted (blue) and reflected (red) intensity of the laser as its frequency is scanned, showing a maximum transmission of 81% through the ring resonator and a finesse of 22. P_2 refers to the second polarization mode passing through the ring resonator. (b) Close up on a single resonance peak. From fitting to the data using Eqs. 1 and 2 with no other free parameters, a value of $\mathcal{V} = 0.987$ is extracted. Points correspond to data and dashed lines correspond to a fit with Eqs. 1 and 2, with the intensity normalised to maximum reflection.

We experimentally characterize the important properties of the ring resonator - namely peak transmission, full-width-at-half-maximum (FWHM), and free spectral range (FSR) - by scanning the piezo-electric transducer of a 1560 nm single-frequency fiber laser (NKT Photonics Koheras BASIK) across resonance. The results obtained are shown in Fig. 2, with the scan range of the laser calibrated by sending the laser output to a wave-meter. We measure an on-resonance transmission of 81%, FWHM of 3 MHz and FSR of 66 MHz, giving a finesse of 22. A fit of this data to Eqs. 1 and 2 with $R = 0.9$ allowed us to determine a DC efficiency of $\mathcal{V} = 0.987$ (i.e., a 1.3% loss in intensity per DC) in agreement with manufacturers specifications. As has been

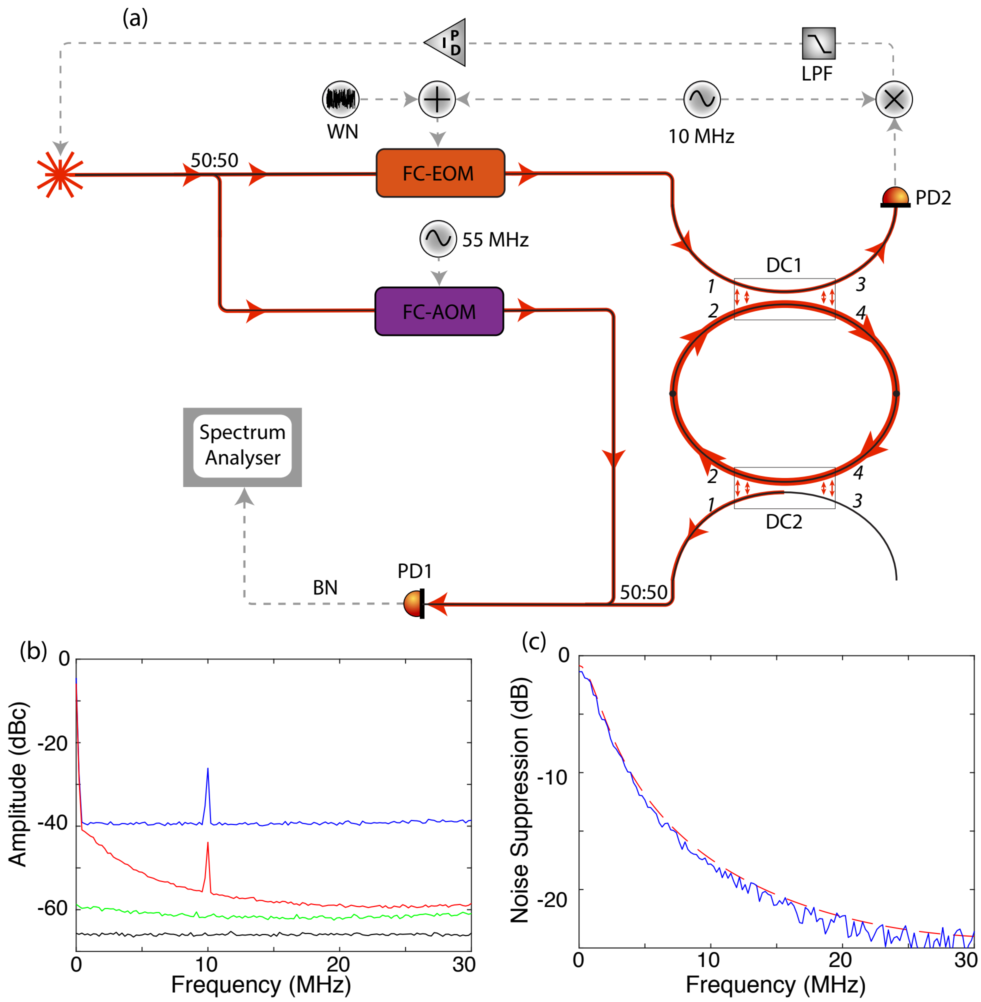

Fig. 3. (a) Experimental apparatus for characterising the noise suppression properties of the ring resonator. DC = Directional coupler; FC-AOM = Fiber-coupled acousto-optic modulator; FC-EOM = Fiber-coupled electro-optic modulator; PID = Proportional-Integral-Derivative controller; LPF = low-pass filter; WN = White noise; PD = Photo diode; BN = Beat note; 50:50 = Non-polarizing fiber beam splitter. (b) Noise spectra of the laser before (blue) and after (red) transmission through the ring resonator centred about the 55 MHz beat frequency. The 10 MHz peaks are a result of the locking modulation. Dark noise (black) and residual amplitude modulation (green) are also shown. (c) Suppression through the ring resonator calculated from experimental data (blue), and from Eq. 2 with $\mathcal{V} = 0.987$ (red).

OSA CONTINUUM

seen previously in other fiber ring resonators [26], by using polarization-maintaining couplers we maintain the input polarization mode of the light as it propagates around the loop. This ensures that very little power will be transferred to the orthogonal polarization mode (P_2 in Fig. 2(a), 28:1 suppression ratio), improving output power stability.

We verified the spectral noise suppression properties of this ring resonator using the experimental set-up illustrated in Fig. 3(a). A fiber-coupled electro-optic modulator (EOM) was inserted at the output of the laser to add white noise to our laser signal with a bandwidth of 60 MHz. The noise on the incident and transmitted laser signals was measured by mixing the laser with a local oscillator, shifted 55 MHz from the carrier by an acousto-optic modulator (AOM). The beat note was monitored using an RF spectrum analyser. To stabilize the laser to the ring resonator during these measurements we also added 10 MHz phase modulation side-bands onto the light with the EOM. We then mixed down the signal received at the reflection port with another 10 MHz source, phase-locked to the first, followed by low-pass filtering (Fig. 3(a)). This allowed us to use the Pound-Drever-Hall technique [27] to stabilize the laser wavelength to the ring resonator via a Proportional-Integral-Derivative controller (New Focus B1005) to the laser's piezo-electric transducer.

Figure 3(b) shows the noise spectrum of the laser before (blue) and after (red) being transmitted through the fiber ring resonator centred about the 55 MHz beat frequency. The dark noise of the photodetector (black) and the residual amplitude modulation (RAM) of the transmitted laser (green) were measured by blocking all light signals from the photodiode, and by eliminating the local oscillator signal from the photodiode respectively. As the level of white noise used ensured that the transmitted noise was always above the dark noise even at maximum suppression, we could accurately determine the suppression behavior of the ring resonator by measuring the ratio of the noise between the incident and transmitted signals. The result of this calculation is shown on Fig. 3(c) (blue) along with the expected noise suppression derived from Eq. 2 using the ring resonator parameters we have determined previously (red). We removed the confounding effects of RAM by subtracting it (in quadrature) from the transmitted noise signal. The maximum suppression is seen to be 25 dB at 30 MHz, the point midway between the resonant modes.

4. Discussion

Given the promising results achieved above it is worth considering some of the limitations of such technology.

Firstly, the major power limitation for a fiber-based ring resonator is Stimulated Brillouin Scattering (SBS). The threshold power for SBS can be calculated as approximately 1.2 W for the optical fiber in this ring resonator [28], which with $\mathcal{F} = 22$ corresponds to an input power limit of approximately 150 mW. A number of techniques have been developed to suppress SBS in optical fibers in the pursuit of high power single frequency laser amplification. One common method for reducing effective SBS gain is to use a thermal gradient along the fiber to create a spatially varying Stokes shift, resulting in inhomogeneous broadening [29,30]. SBS can also be mitigated by reducing the overlap of sound waves and circulating light fields by using specially tailored fibers [31]. Another approach is to use fibers with larger mode field diameters [32], with one specially designed large-core single-mode fibre demonstrating the ability to transmit 500 W of single-frequency light [33]. With this level of circulating power, a fiber ring resonator with the specifications determined above would be able to produce approximately 50 W of power at its output, enough to seed the high power oscillator stage of the current advanced Laser Interferometer Gravitational-wave Observatory (aLIGO) [34].

A second issue that must be considered is that a fiber resonator, like all resonators, will still transmit noise at integer multiples of the FSR. However, most experiments only require suppression at key measurement frequencies. For instance, in the aLIGO detector the three RF sideband frequencies that are used to generate error signals for controlling the auxiliary degrees of freedom, and where noise suppression is important, are 9, 36 and 45 MHz [35]. This can be achieved by chaining two fiber ring resonators together, as shown in Fig. 4(a), as a resonator with an FSR of 18 MHz will maximally suppress noise at both 9 and 45 MHz (Fig. 4(b)(i)). As can be seen from Fig. 4(b)(iii) we can achieve at least 27 dB of suppression for 36 MHz and up to 50 dB suppression at 45 MHz with over 60% of the resonant light transmitted. These levels of targeted filtering compare favourably with the current aLIGO mode-cleaner (with a finesse of 500 and FSR of 9 MHz [35]), producing 50 dB of suppression at 4.5 MHz, and would allow the finesse of this final mode-cleaner to be lowered for future designs, with a corresponding decrease in maximum circulating power.

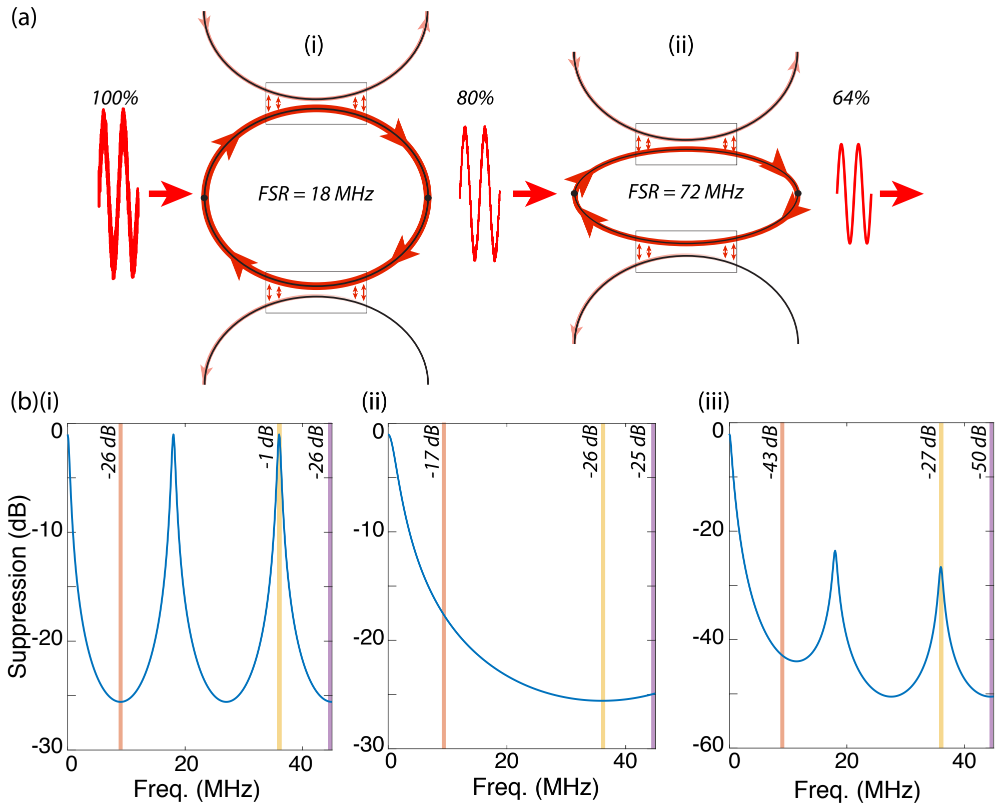

Fig. 4. (a) Chaining arrangement required to suppress noise at key GW detection frequencies using two fibre ring resonators with free-spectral ranges of (i) 18 MHz and (ii) 72 MHz. Percentages show amount of the input light at each point in the chain. (b) Calculated suppression through ring resonators (i) and (ii), as well as (iii) the total suppression for the system. Colored bands show key GW control frequencies with corresponding amount of suppression.

A third issue to consider is the stability of this type of ring resonator. The fiber resonator will be sensitive to changes in temperature which, in turn, affects the optical path length with an expected shift of approximately 8 fringes per degree [36]. As the temperature of this type of resonator can be readily kept stable to the 10 mK level we would expect a drift from resonance frequency of order 5 MHz, corresponding to a drop in transmitted power of 95%. Adding active stabilisation with a piezo-electric transducer [37] would be able to compensate for this effect, with a change in resonator length of under a micron required to return it to resonance [38]. The

OSA CONTINUUM

available reflection port of the 2 DC fiber ring resonator presented here makes this a convenient option.

Finally, we must consider the achievable finesse from this type of ring resonator due to intra-cavity losses associated with the imperfections of the DCs used. We note that while the commercial DCs used here had a loss of over 1%, custom DCs have demonstrated losses down to 0.1% [20], which would provide a significant positive impact on both the transmission and finesse. Figure 5(a) shows the effect that reducing the loss has on the maximum transmission through the ring resonator as a function of reflectivity of the DCs using Eq. 2. This shows that reducing the loss from 1% to 0.1% would increase maximum transmission to over 98% assuming negligible splice loss. Even with a splice loss equal to or slightly greater than the lowest DC loss, nearly 95% of the light will be transmitted. Reducing the losses within the ring resonator also allows for higher reflectivity DCs to be used without significant reductions in maximum transmission, leading to an increase in finesse and a corresponding increase in the maximum suppression possible (Fig. 5(b)). With these improved characteristics, fiber ring resonators could find additional applications in quantum optics experiments, for instance for the combination or separation of optical fields with similar wavelengths [39]. Incorporating a waveguide-based source of squeezing [40] would also allow for the creation of a new type of fiber-optical parametric oscillator for use in fiber-based quantum information networks. As is the case with classical signals, high circulating power could lead to undesirable effects such as increased phase noise via Brillouin [41] and Raman [42] scattering.

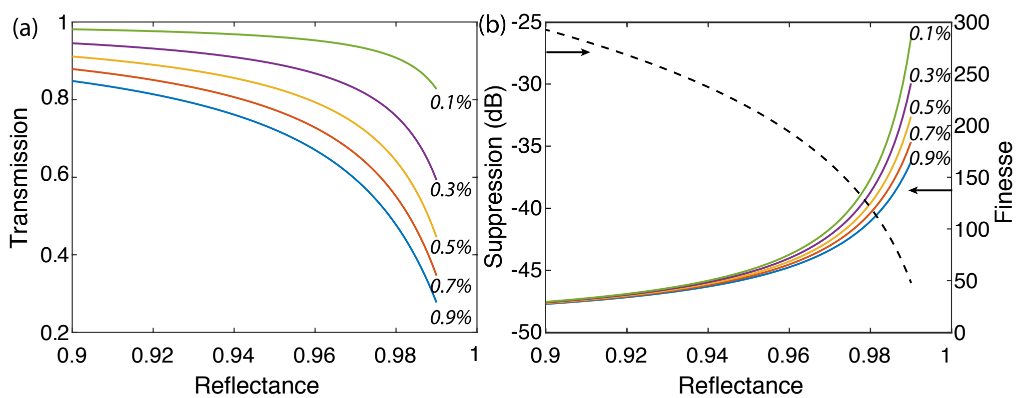

Fig. 5. (a) Simulated ring resonator peak transmission and (b) finesse (solid lines) and maximum suppression (dashed line) as a function of DC reflectivity for a number of different DC loss values. Arrows indicate corresponding axes.

5. Conclusion

In conclusion, we have characterized an all-fiber ring resonator by splicing the end ports of two commercially-available, polarization-maintaining, single-mode, optical fiber directional couplers to form a loop. This type of ring resonator, with 80% transmission and noise suppression of 25 dB is ideal for rugged, robust and compact all-fiber MOPA systems that can deliver high power, low noise output signals. By decreasing the effects of stimulated Brillouin scattering, this ring resonator could provide an all-fiber alternative to the low-power amplifier stage of current gravitational-wave interferometers, and reduce the noise suppression requirements of the final free-space mode-cleaner.

OSA CONTINUUM

Funding

Australian Research Council (CE170100004, DE170100752, DP130104129, LP1410100589).

Acknowledgements

This research was conducted jointly under the ARC Centre of Excellence for Gravitational Wave Discovery(OzGrav) and the Institute for Photonics & Advanced Sensing (IPAS). Product specifications are for clarity only.

References

1. G. W. Matthew O'Toole and D. B. Lindell, "Confocal non-line-of-sight imaging based on the light-cone transform," Nature **555**(7696), 338–341 (2018).
2. H. M. Oubei, J. R. Duran, B. Janjua, H.-Y. Wang, C.-T. Tsai, Y.-C. Chi, T. K. Ng, H.-C. Kuo, J.-H. He, M.-S. Alouini, G.-R. Lin, and B. S. Ooi, "4.8 Gbit/s 16-QAM-OFDM transmission based on compact 450-nm laser for underwater wireless optical communication," Opt. Express **23**(18), 23302 (2015).
3. H. Kaushal and G. Kaddoum, "Optical Communication in Space: Challenges and Mitigation Techniques," IEEE Commun. Surv. Tutorials **19**(1), 57–96 (2017).
4. E. Agrell, M. Karlsson, A. R. Chraplyvy, D. J. Richardson, P. M. Krummrich, P. Winzer, K. Roberts, J. K. Fischer, S. J. Savory, B. J. Eggleton, M. Secondini, F. R. Kschischang, A. Lord, J. Prat, I. Tomkos, J. E. Bowers, S. Srinivasan, M. Brandt-Pearce, and N. Gisin, "Roadmap of optical communications," J. Opt. **18**(6), 063002 (2016).
5. M. F. Brandl, M. W. van Mourik, L. Postler, A. Nolf, K. Lakhmanskiy, R. R. Paiva, S. Möller, N. Daniilidis, H. Häffner, V. Kaushal, T. Ruster, C. Warschburger, H. Kaufmann, U. G. Poschinger, F. Schmidt-Kaler, P. Schindler, T. Monz, and R. Blatt, "Cryogenic setup for trapped ion quantum computing," Rev. Sci. Instrum. **87**(11), 113103 (2016).
6. N. Friis, O. Marty, C. Maier, C. Hempel, M. Holzäpfel, P. Jurcevic, M. B. Plenio, M. Huber, C. Roos, R. Blatt, and B. Lanyon, "Observation of Entangled States of a Fully Controlled 20-Qubit System," Phys. Rev. X **8**(2), 021012 (2018).
7. Instrument Science White Paper, LIGO Document T1700231-v2.
8. G. Guiraud, N. Traynor, and G. Santarelli, "High-power and low-intensity noise laser at 1064nm," Opt. Lett. **41**(17), 4040 (2016).
9. S. Xu, Z. Yang, T. Liu, W. Zhang, Z. Feng, Q. Zhang, and Z. Jiang, "An efficient compact 300 mW narrow-linewidth single frequency fiber laser at 1.5 μm," Opt. Express **18**(2), 1249 (2010).
10. S. Saraf, S. Sinha, A. K. Sridharan, and R. L. Byer, "100 w, single frequency, low-noise, diffraction-limited beam from an nd:yag end-pumped slab mopa for ligo," Advanced Solid-State Photonics, Optical Society of America, 2004, p. PDP15.
11. Pre-Stabilized Laser Design, LIGO Document T050036-00-P.
12. B. Willke, N. Uehara, E. K. Gustafson, R. L. Byer, P. J. King, S. U. Seel, and R. L. Savage, "Spatial and temporal filtering of a 10-W Nd:YAG laser with a Fabry–Perot ring-cavity premode cleaner," Opt. Lett. **23**(21), 1704 (1998).
13. J. Zhao, G. Guiraud, C. Pierre, F. Floissat, A. Casanova, A. Hreibi, W. Chaibi, N. Traynor, J. Boullet, and G. Santarelli, "High-power all-fiber ultra-low noise laser," Appl. Phys. B: Lasers Opt. **124**(6), 114 (2018).
14. P. Kwee, C. Bogan, K. Danzmann, M. Frede, H. Kim, P. King, J. Pöld, O. Puncken, R. L. Savage, F. Seifert, P. Wessels, L. Winkelmann, and B. Willke, "Stabilized high-power laser system for the gravitational wave detector advanced LIGO," Opt. Express **20**(10), 10617 (2012).
15. Y. O. Barmenkov, D. Zalvidea, S. Torres-Peiró, J. L. Cruz, and M. V. Andrés, "Effective length of short Fabry-Perot cavity formed by uniform fiber Bragg gratings," Opt. Express **14**(14), 6394 (2006).
16. J. H. Chow, D. E. McClelland, M. B. Gray, and I. C. Littler, "Demonstration of a passive subpicostrain fiber strain sensor," Opt. Lett. **30**(15), 1923 (2005).
17. F. Zhang and J. W. Lit, "Direct-coupling single-mode fiber ring resonator," J. Opt. Soc. Am. A **5**(8), 1347 (1988).
18. L. F. Stokes, M. Chodorow, and H. J. Shaw, "All-single-mode fiber resonator," Opt. Lett. **7**(6), 288 (1982).
19. R. E. Meyer, S. Ezekiel, D. W. Stowe, and V. J. Tekippe, "Passive fiber-optic ring resonator for rotation sensing," Opt. Lett. **8**(12), 644 (1983).
20. D. B. H. Ming and H. Yu, "Low Loss Fiber Ring Resonator," Proc. SPIE **0478**, 104 (1984).
21. P. Urquhart, "Compound optical-fiber-based resonators," J. Opt. Soc. Am. A **5**(6), 803–812 (1988).
22. Y. H. Ja, "Generalized theory of optical fiber loop and ring resonators with multiple couplers. 2: General characteristics," Appl. Opt. **29**(24), 3524–3529 (1990).
23. P. H. Merrer, O. Llopis, and G. Cibiel, "Laser Stabilization on a Fiber Ring Resonatorand Application to RF Filtering," IEEE Photonics Technol. Lett. **20**(16), 1399–1401 (2008).
24. K. Saleh, J. Millo, B. Marechal, B. Dubois, A. Bakir, A. Didier, C. Lâcroute, and Y. Kersalé, "Photonic Generation of High Power, Ultrastable Microwave Signals by Vernier Effect in a Femtosecond Laser Frequency Comb," Sci. Rep. **8**(1), 1997 (2018).
25. N. Hodgson and H. Weber, *The Fabry Perot Resonator* (Springer, 1997) pp. 137–162.

OSA CONTINUUM

26. T. Feng, D. Ding, F. Yan, Z. Zhao, H. Su, and X. S. Yao, "Widely tunable single-/dual-wavelength fiber lasers with ultra-narrow linewidth and high OSNR using high quality passive subring cavity and novel tuning method," Opt. Express **24**(17), 19760–19768 (2016).
27. E. D. Black, "An introduction to Pound-Drever-Hall laser frequency stabilization," Am. J. Phys. **69**(1), 79–87 (2001).
28. R. Boyd, *Nonlinear Optics* (Elsevier Science, 2003).
29. M. W. Zmda, "Stimulated Brillouin Scattering (SBS) Suppression Techniques," Technical Report, Airforce Research Laboratory AFRL-DE-PS-TR-2007-1127 (2007).
30. Y. Wang, C.-Q. Xu, and H. Po, "Thermal effects in kilowatt fiber lasers," IEEE Photonics Technol. Lett. **16**(1), 63–65 (2004).
31. S. Gray, D. T. Walton, X. Chen, J. Wang, M.-J. Li, A. Liu, A. Ruffin, J. A. Demeritt, and L. A. Zenteno, "Optical fibers with tailored acoustic speed profiles for suppressing stimulated Brillouin scattering in high-power, single-frequency," IEEE J. Sel. Top. Quantum Electron. **15**(1), 37–46 (2009).
32. Y. Imai and N. Shimada, *Dependence of Gain Spectrum and Threshold in SBS on Temperature Distribution in Fibers* (Springer, US, 1995).
33. S. Gray, A. Liu, D. T. Walton, J. Wang, M.-J. Li, X. Chen, A. B. Ruffin, J. A. DeMeritt, and L. A. Zenteno, "502 Watt, single transverse mode, narrow linewidth, bidirectionally pumped Yb-doped fiber amplifier," Opt. Express **15**(25), 17044 (2007).
34. Instrument Science White Paper, LIGO Document P1400177-v5.
35. J. Aasi, *et al.*, "Advanced LIGO," Classical Quantum Gravity **32**(7), 074001 (2015).
36. T. S. Priest, K. T. Jones, G. B. Scelsi, and G. A. Woolsey, "Thermal Coefficients of Refractive Index and Expansion in Optical Fibre Sensing," *Proc. 12th Int. Conf. Opt. Fiber Sensors*, OWC41, (1997).
37. J. Zhang, C.-Y. Yue, G. W. Schinn, W. R. L. Clements, and J. W. Y. Lit, "Stable single-mode compound-ring erbium-doped fiber laser," J. Lightwave Technol. **14**(1), 104–109 (1996).
38. A. Bertholds and R. Dandliker, "Determination of the individual strain-optic coefficients in single-mode optical fibres," J. Lightwave Technol. **6**(1), 17–20 (1988).
39. M. Hosseini, B. M. Sparkes, G. Campbell, P. K. Lam, and B. Buchler, "High efficiency coherent optical memory with warm rubidium vapour," Nat. Commun. **2**(1), 174 (2011).
40. F. Kaiser, B. Fedrici, A. Zavatta, V. D'Auria, and S. Tanzilli, "A fully guided-wave squeezing experiment for fiber quantum networks," Optica **3**(4), 362 (2016).
41. R. M. Shelby, M. D. Levenson, and P. W. Bayer, "Guided acoustic-wave Brillouin scattering," Phys. Rev. B **31**(8), 5244–5252 (1985).
42. F. X. Kärtner, D. J. Dougherty, H. A. Haus, and E. P. Ippen, "Raman noise and soliton squeezing," J. Opt. Soc. Am. B **11**(7), 1267 (1994).